AIAA JOURNAL
Vol. 38, No. 9, September 2000

Unsteady Leading-Edge Suction Effects on Rotor-Stator Interaction Noise

Johan B. H. M. Schulten*
National Aerospace Laboratory NLR, 8300 AD Emmeloord, The Netherlands

A strictly linear analysis of the sound generated by an unleaned stator yields a vanishing amplitude for modes with zero circumferential periodicity. In such a case higher-order effects become relevant. In the present study the higher-order effect of stator leading-edge suction on radiated sound is addressed. By a local analysis in the vicinity of the leading edge, a suction force can be restored from the first-order theory. This suction force oscillates at twice the frequency of the associated blade loading. Numerical examples show that the effect provides a realistic floor level for the sound that otherwise would seem to vanish. For non-zero circumferential modal wave numbers, the effect can increase the acoustic intensity by as much as 10 dB.

Nomenclature

B = number of blades or vanes in row considered
C_T = tangential force coefficient [Eq. (24)]
c = blade (or vane) chord
D = angular position of zeroth vane [Eq. (4)]
$\tilde{G}$ = Green's function [Eq. (3)]
h = hub/tip ratio
$\boldsymbol{i}_x, \boldsymbol{i}_r, \boldsymbol{i}_\theta$ = unit vectors in x, r, θ directions
k = circumferential periodicity of incident velocity
M = axial flow Mach number
p = pressure induced by blade row
r = radial coordinate
t = time coordinate
U = local parallel flow velocity [Eq. (9)]
$U_{m\mu}$ = radial eigenfunction [Eq. (4)]
$\boldsymbol{v}$ = velocity induced by blade row
w = streamwise wake velocity
x = axial coordinate along duct axis
β = $\sqrt{(1 - M^2)}$
γ = corner flow magnitude [Eq. (9)]
Δp = blade pressure jump distribution [Eq. (4)]
ε = small parameter [Eq. (7)]
$\varepsilon_{m\mu}$ = radial eigenvalue [Eq. (5)]
θ = circumferential coordinate, argument [Eq. (10)]
ξ = axial source coordinate
$\boldsymbol{\xi}$ = source position vector [Eq. (3)]
ρ = radial source coordinate, mass density
τ = source time [Eq. (3)]
ϕ = circumferential source coordinate, phase angle
ω = Helmholtz number (nondimensional frequency)
$\langle \cdot \rangle$ = inner product of three-dimensional vectors

Subscripts

L = leading edge
m = merging
s = suction
T = trailing edge, tangential
w = wake
∞ = at infinity

Superscripts

(a) = anechoic
$+$ = blade lower side, downstream
$-$ = blade upper side, upstream
$*$ = complex conjugate
$\sim$ = in time domain

Received 30 April 1999; presented as Paper 99-1951 at the AIAA/CEAS 5th Aeroacoustics Conference, Seattle, WA, 10–12 May 1999; revision received 14 January 2000; accepted for publication 14 January 2000.

*Senior Research Engineer, Aeroacoustics Department, P.O. Box 153; schulten@nlr.nl. Senior Member AIAA.

Introduction

PROBABLY the most important step forward in the history of fan noise research has been Tyler and Sofrin's[1] study on the role of blade and vane numbers in noise generation. They showed that for a fan rotating with a subsonic tip speed it is straightforward to suppress the fundamental blade passing frequency (first harmonic) by choosing a sufficiently high number of stator vanes. Then, all acoustic duct modes become cutoff and do not propagate along the duct. In aeronautical practice "sufficiently high" turns out to be about twice the number of rotor blades.

In an idealized model the duct mean flow is uniform and the acoustic perturbations are small. Corresponding blade rows are aligned with the relative mean flow and thus lack mean loading. Then, the expression for the modal amplitudes generated by the impingement of rotor wakes on a stator shows that amplitudes are proportional to the circumferential mode number m. According to Tyler and Sofrin's[1] selection rule we obtain $m = 0$ in the second harmonic when the stator vane number is exactly twice the rotor blade number. This would result in a zero amplitude. Of course, this looks too good to be true and, as shown earlier,[2] higher-order effects such as realistic vane camber and stagger angle become significant under such circumstances.

However, even with an idealized geometry, the acoustic intensity will not vanish because of another nonlinear, higher-order phenomenon: the presence of a vane leading-edge suction force, oscillating because of incident flow distortions. For isolated airfoils the existence of such a suction force was reported by Katzmayr[3] in 1922. His experiments were rather focused on the time-averaged component of this suction that produces a negative airfoil drag under favorable conditions. More recently, Ribner[4] analyzed the single flat plate airfoil problem theoretically for incompressible flow. He clearly pointed out that, apart from a steady component, the suction thrust oscillates about a mean at twice the frequency of the incident upwash field. Amiet[5] extended the solution to a flat plate airfoil in a subsonic flow. His analysis is the most relevant for the present work, which is concerned with the acoustic effects of the leading-edge suction of a complete stator.

Theoretical Modeling

Governing Equations

In the present study a lifting surface, i.e., linearized and inviscid modeling of the rotor-wake/stator interaction, will be used. A lifting surface modeling of a flow problem is based on two assumptions. First, the viscosity of the flow is considered to be small, i.e., the Reynolds number is assumed to be sufficiently high. Second, the

perturbations of the main flow caused by the presence of the blades are supposed to be relatively small.

We consider a single blade row placed in a uniform, subsonic main flow of Mach number $M(0 < M < 1)$. To obtain a nondimensional formulation, the mass density and speed of sound of the main flow and the duct radius are taken as scaling parameters. With this scaling, the pressure and density perturbation become to leading order identical. The governing, i.e., the leading order, flow equations are the linearized Euler equations for the (dimensionless) perturbation pressure $\tilde{p}$ and velocity $\tilde{\mathbf{v}}$:

$$\frac{\mathrm{D}\tilde{p}}{\mathrm{D}t} + \langle \nabla \cdot \tilde{\mathbf{v}} \rangle = 0 \tag{1}$$

$$\frac{\mathrm{D}\tilde{\mathbf{v}}}{\mathrm{D}t} + \nabla \tilde{p} = \mathbf{0} \tag{2}$$

where a tilde indicates that the variable is understood to be in the time domain. If the x axis is chosen along the duct axis the linearized material derivative $\mathrm{D}/\mathrm{D}t = \partial/\partial t + M\partial/\partial x$.

Stator Sound Field

As shown previously,[6,7] application of generalized functions to make Eqs. (1) and (2) formally valid throughout space, i.e., also within the blades, and elimination of the velocity yields a nonhomogeneous convected-wave equation in the pressure. The right-hand side of this equation consists of two source terms, one of which contains the blade loading distribution and the other the blade thickness distribution. It appears that the latter only affects the steady blade response and plays no role in the wake interaction problem. After the construction of Green's function $\tilde{G}$ for this equation in terms of a multiple Fourier transform, the wake interaction pressure field of a stator can be expressed as the following integral over the source volume and time:

$$\tilde{p} = \iiiint \langle \nabla_0 \tilde{G} \cdot \nabla S \rangle \tilde{p}\, \delta(S)\, \mathrm{d}\boldsymbol{\xi}\, \mathrm{d}\tau \tag{3}$$

where ∇_0 denotes the gradient operator with respect to the source coordinates $\boldsymbol{\xi}$. Following Ffowcs Williams and Hawkings,[7] S is a smooth function that defines the vane surfaces through $S > 0$ outside and $S < 0$ inside the vanes. This pressure field contains unsteady components at multiples of the rotor wakes passing frequency. Upon substitution of the pressure field, the momentum equation yields expressions for the velocity induced by the vane loading. After omitting the higher-order terms in the geometry, upper and lower surface pressure reduce into the pressure jump Δp across the vanes.

Integral Equation

To solve the unknown pressure jump distribution Δp we have to apply the boundary condition of flow tangency at the vane surfaces. By splitting the incident field of rotor wakes into circumferential Fourier components, the integral equation becomes identical for all vanes of the stator. Combining the boundary conditions at upper and lower blade surfaces as in Ref. 6, we obtain an integral equation for Δp because of an incident velocity field. The numerical method to solve this integral equation is described in Refs. 8 and 9.

Modal Amplitudes

Green's function $\tilde{G}$ can be considered as the sound field of an impulsive point source. For a duct $\tilde{G}$ takes the form of an expansion in acoustic modes.[9] For unswept, unleaned vanes, the resulting pressure field at a single frequency can be written as

$$\tilde{p}(x, r, \theta, t) = \frac{-B}{2\pi} \exp(i\omega t) \sum_{n=-\infty}^{\infty} \exp[im(\theta - D)] m \sum_{\mu=1}^{\infty} \frac{U_{m\mu}(r)}{2\beta_{m\mu}(\omega)}$$

$$\times \int_h^1 \frac{U_{m\mu}(\rho)}{\rho} \int_{x_L}^{x_T} \exp\left[i \frac{(x-\xi)}{\beta^2} [M\omega - \mathrm{sgn}(x-\xi)\beta_{m\mu}(\omega)] \right]$$

$$\times \Delta p(\xi, \rho)\, \mathrm{d}\xi\, \mathrm{d}\rho \tag{4}$$

where the circumferential wave number $m = k - nB$ and

$$\beta_{n\mu} = \omega\sqrt{1 - (\varepsilon_{n\mu}\beta/\omega)^2} \qquad \text{if} \qquad (\varepsilon_{n\mu}\beta)^2 \le \omega^2$$

$$\beta_{n\mu} = -i\sqrt{(\varepsilon_{n\mu}\beta)^2 - \omega^2} \qquad \text{if} \qquad (\varepsilon_{n\mu}\beta)^2 > \omega^2 \tag{5}$$

It is well known[1] that, for a given frequency ω, only a finite number of modes actually propagates along the duct. In practice it is quite feasible to select blade and vane numbers such that in the blade passing frequency (first harmonic) all modes are cutoff, i.e., not propagating. Similarly, in many practical cases only a single term of the n series is propagating in the second harmonic. If the corresponding m for this term can be made zero, no sound will radiate in this frequency.

However, at this point it is to be remembered that the present analysis is concerned with the leading term of an asymptotic analysis in the small perturbation parameter. Therefore, higher-order terms have to be taken into account if the leading term vanishes. For instance, it should be noted that the vane geometry is to leading order approximated by flat plates parallel to the axial mean flow. In an earlier study[2] the higher-order effect of vane camber and stagger was shown to become significant in the case of high frequencies and low m. In this paper it is shown that even with a truly flat geometry the sound will not vanish when $m = 0$.

Leading-Edge Suction Force

Vanes are designed to operate under a wide range of angles of attack in a subsonic flow and therefore have a leading edge sufficiently rounded to sustain a suction force in the forward direction. In principle the leading-edge suction force is a higher-order effect not captured by the lifting surface approximation, which accommodates only forces normal to the lifting surface. In a recent study on an airfoil traveling through a sinusoidal upwash field, Amiet[5] recovered the suction force first for a steady flow from D'Alembert's paradox (zero drag in steady, inviscid two-dimensional flow). Then, following von Kármán and Burgers,[10] he argued that in an unsteady flow the suction force is a very local phenomenon that may be considered as quasi-steady. Consequently, the result obtained for steady flow should also apply to unsteady flow. Here we will follow a more general, asymptotic approach basically valid for the flow in the immediate vicinity of any subsonic leading edge.

Let (x, y, z) be a local Cartesian frame with its origin at the leading edge, x aligned with the main flow direction, y normal to vane surface (no lean is considered), and z in the spanwise direction. Then, the equation for the perturbation potential induced by the vane reads

$$\beta^2 \frac{\partial^2\phi}{\partial x^2} + \frac{\partial^2\phi}{\partial y^2} + \frac{\partial^2\phi}{\partial z^2} - 2M\frac{\partial^2\phi}{\partial x\,\partial t} - \frac{\partial^2\phi}{\partial t^2} = 0 \tag{6}$$

The flow in the vicinity of the leading edge is characterized by a moving stagnation point. The maximum distance from the leading edge ε of the stagnation point attained during an unsteady cycle therefore is a natural length scale of flow variation in the plane normal to leading edge. Introducing scaled coordinates

$$x = \beta\varepsilon X, \qquad y = \varepsilon Y \tag{7}$$

into Eq. (6) yields

$$\frac{\partial^2\phi}{\partial X^2} + \frac{\partial^2\phi}{\partial Y^2} - 2\varepsilon\frac{M}{\beta}\frac{\partial^2\phi}{\partial X\,\partial t} + \varepsilon^2\left[\frac{\partial^2\phi}{\partial z^2} - \frac{\partial^2\phi}{\partial t^2}\right] = 0 \tag{8}$$

Obviously, close to the leading edge the unsteady perturbation potential is to leading order governed by the two-dimensional Laplace equation, i.e., the flow indeed behaves predominantly quasi-steady and time dependence only appears parametrically. At the same time the geometry of the leading-order problem reduces to a semi-infinite plate because for practical cases ε is much smaller than the vane chord and the wavelength of incoming gusts. Restricting ourselves to the leading order, we can apply classical two-dimensional potential theory in which the flow about a semi-infinite plate is an extreme case of a corner flow, e.g., see Ref. 11, p. 410.

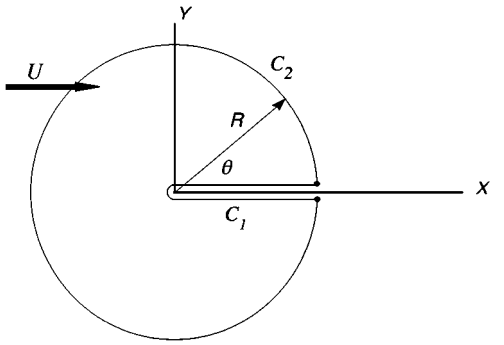

Fig. 1 Integration contours C_1 and C_2 to recover suction force.

The complex potential χ of a semi-infinite plate in a parallel flow $U\boldsymbol{i}_x$ with superimposed corner flow of magnitude γ is given by

$$\chi = U(Z + \gamma\sqrt{Z}) \tag{9}$$

where $Z = X + iY$. Hence the complex conjugate velocity (Fig. 1) is

$$\frac{\mathrm{d}\chi}{\mathrm{d}Z} = u - iv = U\left[1 + \frac{\gamma}{2\sqrt{R}}\exp\left(-i\frac{\theta}{2}\right)\right] \tag{10}$$

The pressure follows from Bernoulli's theorem for incompressible flow

$$p + \tfrac{1}{2}\rho_\infty(u^2 + v^2) = p_\infty + \tfrac{1}{2}\rho_\infty U^2 \tag{11}$$

In general the infinitesimal tangential and normal force components of the pressure acting on a body surface are given by

$$\mathrm{d}T = p\,\mathrm{d}Y, \qquad \mathrm{d}N = -p\,\mathrm{d}X \tag{12}$$

Now consider a contour C_1 wrapped around the plate leading edge (Fig. 1). The force (T, N) acting on the covered part of the plate is then given by

$$T - iN = i\int_{C_1} p\,\mathrm{d}Z^* \tag{13}$$

After some manipulation, e.g., Ref. 11, p. 433, substitution of Eqs. (10) and (11) then yields

$$T - iN = -i\frac{\rho_\infty}{2}\int_{C_1}\left(\frac{\mathrm{d}\chi}{\mathrm{d}Z}\right)^2\mathrm{d}Z \tag{14}$$

Obviously, the integrand has singularities in $Z = (0, 0)$, but because the contour made up by C_1 and C_2 does not enclose any singularity (or cross the branch cut $X \geq 0$, $Y = 0$), we have

$$\int_{C_1}\left(\frac{\mathrm{d}\chi}{\mathrm{d}Z}\right)^2\mathrm{d}Z = -\int_{C_2}\left(\frac{\mathrm{d}\chi}{\mathrm{d}Z}\right)^2\mathrm{d}Z \tag{15}$$

Hence the force on the forward part of the plate can equivalently be calculated from the integration along C_2, which is straightforward. The resulting force (T, N) per unit span is given by

$$T = -\tfrac{1}{2}\rho_\infty U^2(\pi/2)\gamma^2, \qquad N = \tfrac{1}{2}\rho_\infty U^2 4\gamma\sqrt{X} \tag{16}$$

Note that, in contrast to the tangential force, the normal force depends on the covered length from the leading edge. Further, the normal force is linear in the corner flow strength γ, whereas the tangential suction force scales on γ^2.

Application of Bernoulli's theorem [Eq. (11)] along the upper $(-)$ and lower $(+)$ surface of the plate yields

$$\Delta C_p(X) = (p^+ - p^-)\Big/\tfrac{1}{2}\rho_\infty U^2 = 2\gamma/\sqrt{X} \tag{17}$$

Clearly, this relation between Δp and γ is valid for incompressible flow. Because the lifting surface result is for compressible flow, we use the Prandtl–Glauert similarity rule[12] to obtain

$$2\gamma = \sqrt{X}\Delta C_{p_{\mathrm{inc}}}(X) = \beta\sqrt{X}\Delta C_{p_{\mathrm{compr}}}(X)$$
$$= \sqrt{\beta}\lim_{x\downarrow 0}\sqrt{x}\Delta C_{p_{\mathrm{compr}}}(x) \tag{18}$$

Usually the ΔC_p, computed by a lifting surface method, is given as the following Glauert series:

$$\Delta C_p = P_0\tan\frac{\phi}{2} + \sum_{\lambda=1}^{\infty} P_\lambda \sin\lambda\phi \tag{19}$$

where $x = c(1 + \cos\phi)/2$. Now it is easy to show that

$$\lim_{x\downarrow 0}\sqrt{x}\Delta C_{p_{\mathrm{compr.}}}(x) = P_0\sqrt{c} \tag{20}$$

Upon substitution of this result in Eq. (18), we can eliminate γ in Eq. (16) to obtain

$$C_T = T\Big/\tfrac{1}{2}\rho U^2 c = -(\pi\beta/8)P_0^2 \tag{21}$$

which is identical to Amiet's[5] result [his Eq. (6)] but derived in a rather different way.

Frequency Doubling

In the preceding section, a theory for steady flow was applied on a very small length and time scale (in the vicinity of the leading edge) to recover the instantaneous suction force. On the larger scale of the complete blade row, the time dependence of the suction force is imposed by the pressure jump fluctuation at frequency ω. Of course, the suction force also depends on the radial position ρ. Making this dependence explicit by replacing P_0 in Eq. (21) by $|P_0(\rho)|\cos[\omega t + \phi(\rho)]$ we obtain

$$\tilde{C}_T(\rho, t) = -(\pi\beta|P_0(\rho)|^2/8)\{1 + \cos[2\omega t + 2\phi(\rho)]\}/2 \tag{22}$$

As noted by Ribner,[4] this remarkable result shows that the suction force resulting from a pressure jump oscillating at a frequency ω consists of a steady part and a part oscillating with frequency 2ω. Consequently, the first harmonic pressure jump generates a suction force in the second harmonic, the second harmonic pressure jump generates a suction force in the fourth harmonic, and so on.

This is a truly nonlinear effect that is not present in first-order acoustic theories, even in those that account for mean vane loading and nonuniform mean flow. The reason for the frequency doubling is that the suction phenomenon is insensitive to the sign of angle of attack; upwash is as effective as downwash.

Note that this frequency doubling does not occur when the flow separates at the leading edge to form a vortex. In that case the suction analogy[8,13,14] applies with a leading-edge force acting normal to the lifting surface and oscillating at the same frequency as the associated ΔC_p.

To compute the contribution of the suction force in the modal amplitude, we have to go back to the basic Eqs. (1) and (2). As shown in the Appendix, the modal amplitudes generated by the suction force are given by

$$\Delta A^{\pm}_{m\mu} = \frac{B}{4\pi\beta_{m\mu}(\omega)}\frac{M\omega \mp \beta_{m\mu}(\omega)}{\beta^2}\exp(-imD)$$
$$\times\exp\left[-ix_L\frac{M\omega \mp \beta_{m\mu}(\omega)}{\beta^2}\right]\int_h^1 U_{m\mu}(\rho)C_T(\rho)\,\mathrm{d}\rho \tag{23}$$

where

$$C_T(\rho) = -(M^2/2)(\pi\beta c/8)\left[P_0^2(\rho)\Big/2\right] \tag{24}$$

Parametric Study

Configuration

To obtain an idea of the relevance of the suction phenomenon, its effect for a generic modern fan was numerically studied. The characteristics of this fan are listed in Table 1. The stator has vanes with a constant chord, without sweep or lean. The rotor has unswept blades with a constant axial extent aligned with the relative local main flow. In the present study the rotor is considered as an acoustically transparent, viscous wake generator.

To put the analysis in the practical context of noise control, the effect was studied as a function of the axial gap between rotor and stator. Increasing the rotor-stator spacing is an obvious way to reduce interaction noise.

Wake Velocity

Incident rotor blade wakes were computed according to Schlichting's[15] formulas for turbulent wakes in a quasi-two-dimensional way. In a local Cartesian coordinate system (s, q) with the rotor blade trailing edge as origin, the wake velocity is given by

$$w = -\frac{U}{4\sqrt{\pi\lambda}}\sqrt{\frac{c_{dw}c_w}{s}}\exp\left[\frac{-q^2}{4\lambda c_{dw}c_w s}\right] \tag{25}$$

where c_{dw} is the local drag coefficient, c_w the local rotor blade chord, and the empirical coefficient $\lambda = 0.0222$. This wake profile is for isolated wakes and has no definite boundaries. Because we are dealing with a multiblade wake system, wake merging will take place at some downstream location. In anticipation of merging we also consider a periodic cosine velocity profile, satisfying the far-wake momentum relation

$$w = -\frac{U}{2}\sqrt{\frac{c_{dw}c_w}{s}}\left[\cos\left(\frac{2\pi q}{\sqrt{c_{dw}c_w s}}\right) + 1\right] \tag{26}$$

with boundaries

$$q = \pm\tfrac{1}{2}\sqrt{c_{dw}c_w s} \tag{27}$$

Beyond the location where the boundaries of adjacent wakes intersect, the wake width cannot further increase and, again following Schlichting,[15] the next wake profile is adopted

$$w = -\frac{U}{2}\frac{\sqrt{c_{dw}c_w s_m}}{s}\left[\cos\left(\frac{2\pi q}{\sqrt{c_{dw}c_w s_m}}\right) + 1\right] \tag{28}$$

where the subscript m refers to the merging station. Two levels of incident wake strength were investigated: a rotor blade drag coefficient of 0.025 (low) and of 0.050 (high).

Low Drag Rotor Wakes

Figure 2 presents the wake Fourier coefficients of the first and second harmonic at a radius of 0.8 as a function of the axial distance from the rotor trailing edge. It is readily observed that second wake harmonic becomes very small compared to the first harmonic for a moderate gap and beyond. Therefore it is very well possible that the suction effect, which scales on the square of the first harmonic, may become more important for large rotor-stator spacing. In the following all acoustic intensity refers to the second harmonic of the rotor blade passing frequency only. The presumably much weaker third and higher harmonics are not considered.

Table 1 Rotor and stator data

Parameter	Value
Number of rotor blades	23
Number of stator vanes	Variable (45–47)
Hub/tip ratio, h	0.50
Vane chord length	0.12
Axial Mach number	0.32
Rotor tangential tip Mach number	0.75
Axial extent rotor chord	0.15
Rotor blade drag coefficient	0.025/0.05
Nondimensional second harmonic frequency	34.50
Speed of sound (m/s)	340.43
Air density (kg/m^3)	1.225

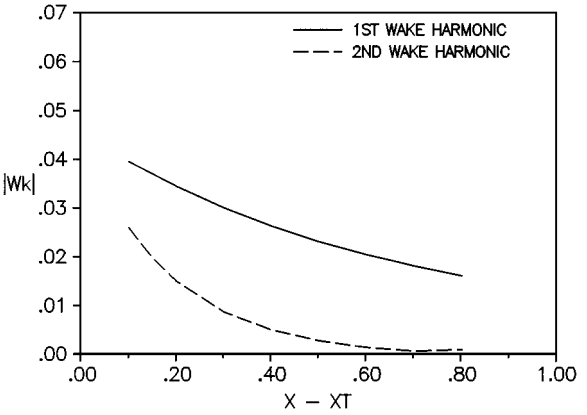

Fig. 2 Absolute value of wake Fourier coefficients, scaled on freestream velocity: rotor blade $c_d = 0.025$, radius = 0.8.

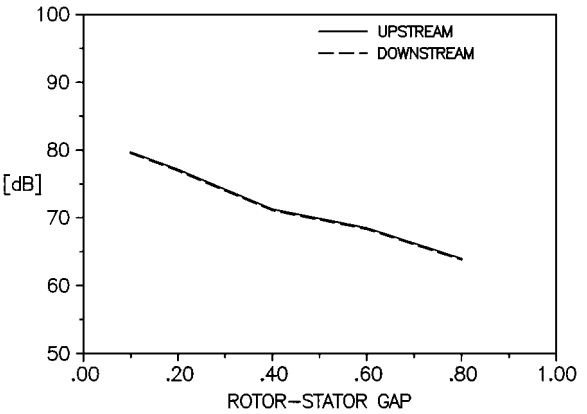

Fig. 3 Acoustic intensity because of leading-edge suction: $m = 0$, 46 vanes, rotor $c_d = 0.025$.

The fan has 23 rotor blades and with a stator of 46 vanes Eq. (4) predicts a vanishing base acoustic level in the second harmonic. Hence the acoustic intensity for this case in Fig. 3 is solely caused by the suction force. It is observed that there is almost no difference between the upstream and downstream intensity. The reason for this is that the first radial mode ($m = 0$, $\mu = 1$) has an eigenvalue $\varepsilon_{m\mu} = 0.0$. The relation between outgoing acoustic intensity $W_{m\mu}$ and the modal amplitudes in an anechoic duct is given by

$$W^{\pm}_{m\mu} = \frac{\pi\beta^4\beta_{m\mu}\left|A^{\pm}_{m\mu}\right|^2}{\omega(1 \mp M\beta_{m\mu}/\omega)^2} \tag{29}$$

e.g., Ref. 16. Substitution of Eq. (23) for the modal amplitude shows that for a zero eigenvalue the upstream and downstream intensities (not the amplitudes) are equal. As the first radial mode is dominating the higher modes by far in this case, the total emitted intensities are also practically equal on both sides of the stator.

The suction noise only weakly decreases as the axial gap between rotor and stator is increased. It takes about a sixfold gap increase to obtain a reduction of 10 dB, which reflects the slow decrease of the first wake harmonic with distance (Fig. 2).

If the number of vanes is increased to 47, cut-on modes with $m = -1$ are generated in the second harmonic. The minus sign indicates that these modes are counter-rotating to the rotor. However, to isolate the suction effects, rotor shielding,[17] although important in practice, was not taken into account in the present analysis. In Fig. 4 the computed upstream acoustic intensity is presented. As can be expected from Fig. 2, for a small gap the suction effect is small, but beyond a gap of 0.4 duct radius, it becomes prominent. A maximum of 9 dB in the suction effect is observed at a gap of 0.6.

As shown in Fig. 5, the base level of the downstream interaction noise is about 6 dB higher than the upstream level. Hence, the suction

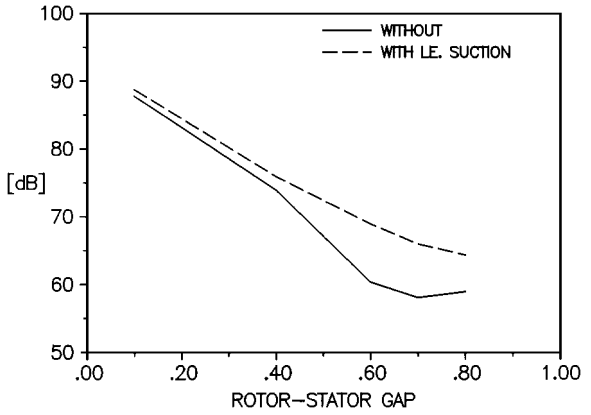

Fig. 4 Upstream intensity, $m = -1$ (47 vanes), rotor $c_d = 0.025$.

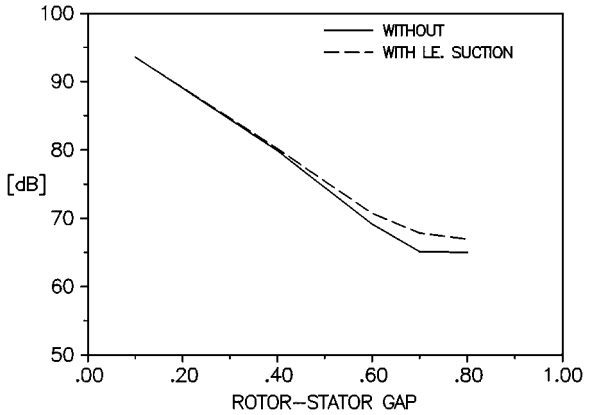

Fig. 5 Downstream intensity, $m = -1$ (47 vanes), rotor $c_d = 0.025$.

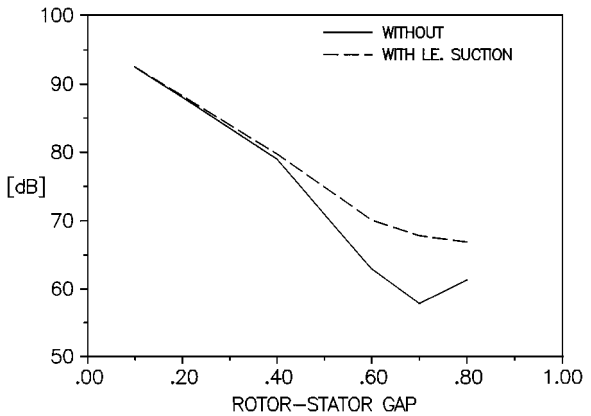

Fig. 6 Upstream intensity, $m = 1$ (45 vanes), rotor $c_d = 0.025$.

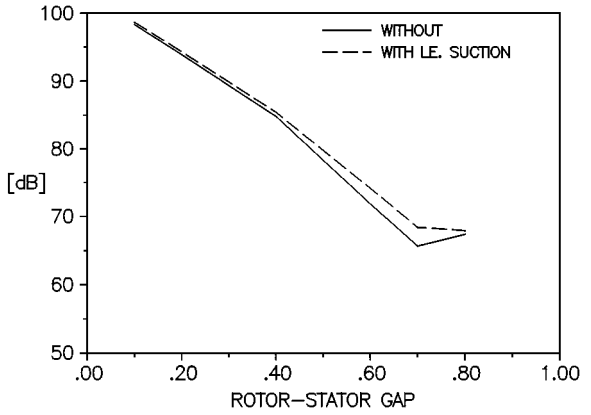

Fig. 7 Downstream intensity, $m = 1$ (45 vanes), rotor $c_d = 0.025$.

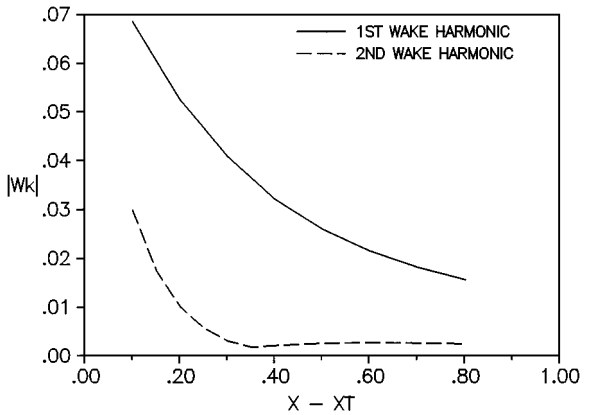

Fig. 8 Absolute value of wake Fourier coefficients, scaled on freestream velocity; rotor $c_d = 0.050$, radius = 0.8.

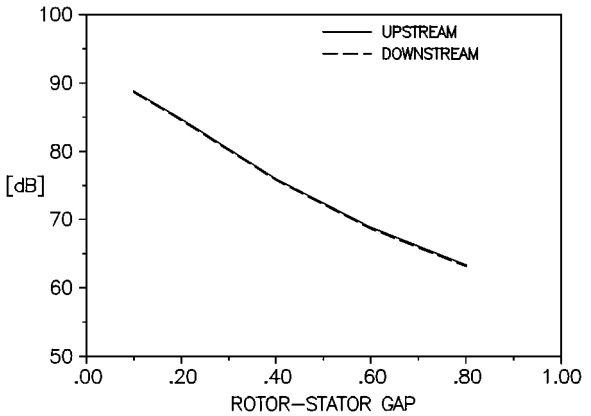

Fig. 9 Effect of increased rotor blade drag ($c_d = 0.05$) on acoustic intensity for $m = 0$ (46 vanes).

effect is relatively weaker than upstream (cf. Fig. 4) and never more than 3 dB, which is still significant, of course.

If the number of vanes is decreased to 45, $m = 1$ modes, rotating in the same sense as the rotor, are generated in the second harmonic. In Fig. 6 the resulting upstream acoustic intensity is given. Despite the slightly lower number of vanes, the base level for a narrow gap is about 5 dB higher than for the $m = -1$ case in Fig. 4. This shows once more how sensitive the acoustic response can be to details one might intuitively ignore. Similar to the $m = -1$ case, the suction effects becomes more important as the gap increases. At a gap of 0.7 the suction effect is 10 dB. The relative increase of the suction effect for a larger gap corresponds to merging of the rotor wakes, which favors the first wake harmonic (Fig. 2). As shown in Fig. 7, the downstream acoustic intensity is modified by suction by 3 dB at most.

High Drag Rotor Wakes

The effect of a larger drag coefficient of the rotor blades is not a simple linear scaling of the incident velocity. As shown by Eqs. (25) and (26), before merging drag affects both the wake velocity and the wake width. The latter is directly connected with the harmonic content of the incident wake system. In Fig. 8 the first and second wake harmonics are plotted as a function of the axial distance from the rotor trailing edge. Indeed, their behavior shows a much steeper gradient for the smaller gaps than in Fig. 2 for the lower drag coefficient. At a gap of 0.4 the amplitude ratio of first and second wake harmonic has a maximum of about 18. Beyond a gap of 0.4 the second wake harmonic is practically constant, whereas the first harmonic is still decreasing.

In Fig. 9 computation shows (cf. Fig. 3) that the suction effect is about 10 dB stronger at a gap of 0.1, whereas the level at a gap of 0.8 has hardly changed. This is not unexpected because a higher drag

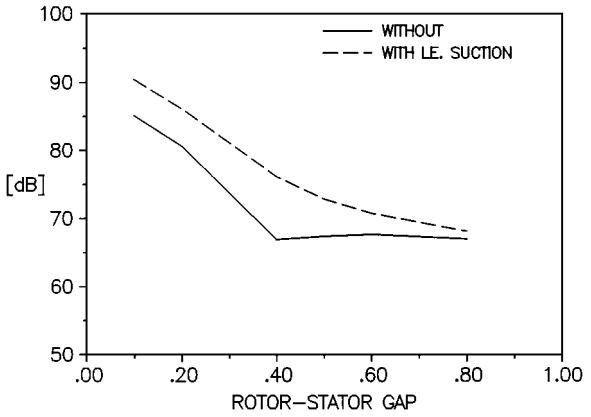

Fig. 10 Upstream intensity, $m = -1$ (47 vanes), rotor $c_d = 0.05$.

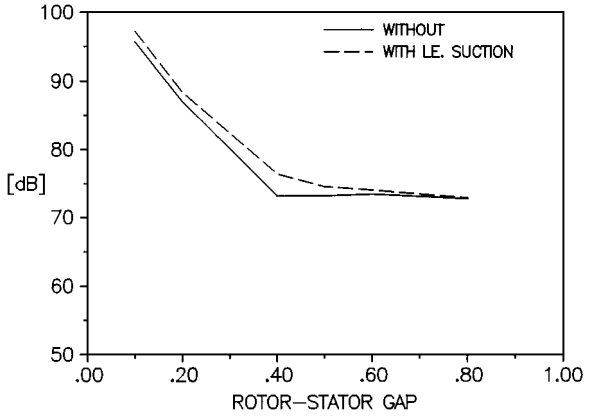

Fig. 11 Downstream intensity, $m = -1$ (47 vanes), rotor $c_d = 0.05$.

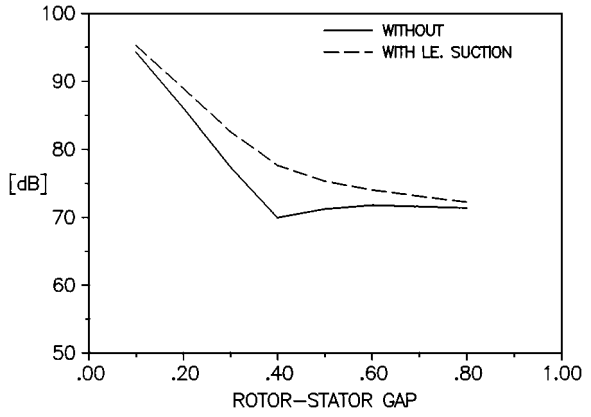

Fig. 12 Upstream intensity, $m = 1$ (45 vanes), rotor $c_d = 0.05$.

coefficient will enhance the first wake harmonic close to the rotor with wider and deeper wakes. At larger distances the first harmonic has undergone more diffusion as a result of an earlier wake merging.

As shown in Fig. 10 (cf. Fig. 4) the increased suction force is quite effective in the upstream intensity for the $m = -1$ case because the base acoustic level has become lower. A suction effect of more than 5 dB at the smallest gap and more than 9 dB at a gap of 0.4 is really significant because a gap below 0.4 is common practice. For a gap larger than 0.4, the suction effect gradually diminishes, which is explained by the decrease of the amplitude ratio in Fig. 8.

The downstream intensity for $m = -1$ is shown in Fig. 11. The suction effect is clearly present but not as spectacular as in the upstream case. Still, an effect of 3 dB at a gap of 0.4 is remarkable because the effect for the low c_d in Fig. 5 is negligible at the same gap. Note also the much steeper initial gradient at which the intensity decreases. Despite a drag coefficient twice as high, this results in a lower noise output in the practically important gap range between 0.2 and 0.5.

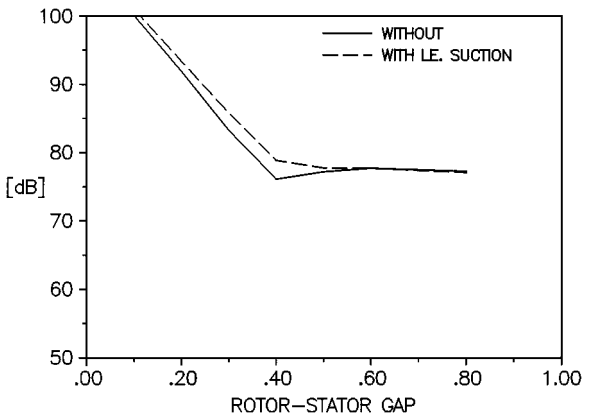

Fig. 13 Downstream intensity, $m = 1$ (45 vanes), rotor $c_d = 0.05$.

The upstream results for 45 vanes ($m = 1$) are shown in Fig. 12. The maximum suction effect is 8 dB at a gap of 0.4. Here also the interaction noise of the high drag rotor is less than the noise of the low drag rotor (Fig. 6) for a gap between 0.2 and 0.5.

Finally, the downstream acoustic intensity in Fig. 13 shows a maximum suction effect of 2.7 dB at a gap of 0.4. Also in this case the gap range 0.2–0.5 is quieter for the high drag rotor (cf. Fig. 7).

Conclusion

An analysis of the acoustic effect of vane leading edge suction has been presented. This effect is a genuinely nonlinear phenomenon that involves frequency doubling. This implies that the suction force associated with the blade passing frequency (1 BPF, usually cutoff) oscillates at twice the blade passing frequency (2BPF, usually cuton). In general the magnitude of the 1BPF wake component is much larger than the 2BPF and this frequency carry over can become quite significant.

It has been outlined how the suction force can be recovered from the first-order lifting surface theory by a local analysis. A numerical study for a generic fan shows that the suction effect provides a realistic bottom level for otherwise vanishing modal amplitudes ($m = 0$). For nonvanishing modal amplitudes ($m \neq 0$), the influence of the suction force tempers the beneficial effect of a large rotor-stator spacing. The suction effect can increase the acoustic intensity by as much as 10 dB.

For low drag rotor wakes the suction effect on acoustic intensity is only significant for rotor-stator gaps larger than 0.4 duct radius. For high drag rotor wakes the suction effect on acoustic intensity is significant for small gaps as well. A maximum effect is observed at a gap of about 0.4.

In general the acoustic effect of suction has a maximum when the vane leading edge is approximately at the wake merging station. For the generic configuration studied, an increase in rotor blade drag can reduce the interaction noise within a certain gap range. This is achieved by the more rapid decrease of the second wake harmonic through an earlier wake merging.

Appendix: Suction Noise Modal Amplitudes

The general derivation of the acoustic field of a body as described in the section "Theoretical Modeling" is not very suitable for the sound field generated by a concentrated line force distribution. Therefore we return to the original linearized Euler equations [Eqs. (1) and (2)], but now we add a point force $\boldsymbol{f}$ acting in space time (ξ, τ) to the right-hand side of the momentum equation. Then, elimination of the velocity yields the following nonhomogeneous convected wave equation for the pressure field of an impulsive point force:

$$\left(\nabla^2 - \frac{\mathrm{D}^2}{\mathrm{D}t^2}\right)\tilde{p}_f = \delta(t-\tau)\langle \boldsymbol{f}\cdot\nabla\,\delta(\boldsymbol{x}-\boldsymbol{\xi})\rangle \qquad \text{(A1)}$$

Because Green's function $\tilde{G}$ for the convected-wave operator by definition satisfies

$$\left(\nabla^2 - \frac{\mathrm{D}^2}{\mathrm{D}t^2}\right)\tilde{G} = -\delta(t-\tau)\delta(\boldsymbol{x}-\boldsymbol{\xi}) \tag{A2}$$

we observe that the sound field of the point force is given by

$$\tilde{p}_f = -\langle \boldsymbol{f}\cdot\nabla\tilde{G}\rangle \tag{A3}$$

in which the expression for $\tilde{G}$ can be found in Ref. 9. After taking the Fourier transform in time of Eq. (A3), substitution of the suction force distribution given by Eq. (24) for $\boldsymbol{f}$ yields

$$p_s = \int_h^1 \langle -\boldsymbol{i}_x C_T(\rho)\cdot\nabla G\rangle \,\mathrm{d}\rho = \int_h^1 C_T(\rho)\frac{\partial G}{\partial \xi}\,\mathrm{d}\rho \tag{A4}$$

Because of the angular separation, the suction force of the jth vane is related to the zeroth vane suction force as follows:

$$C_{T_j} = C_T(\rho)\exp[i2kj(2\pi/B)] \tag{A5}$$

where k denotes the circumferential periodicity of the wake harmonic generating the suction force. Summation over the vanes yields

$$p_s = \frac{B}{2\pi}\sum_{n=-\infty}^{\infty}\exp[im(\theta - D)]\sum_{\mu=1}^{\infty}\frac{U_{m\mu}(r)}{2\beta_{m\mu}}\frac{M\omega - \mathrm{sgn}(x-x_L)\beta_{m\mu}}{\beta^2}$$

$$\times\exp\left[i(x-x_L)\frac{M\omega - \mathrm{sgn}(x-x_L)\beta_{m\mu}}{\beta^2}\right]\int_h^1 U_{m\mu}(\rho)C_T(\rho)\,\mathrm{d}\rho \tag{A6}$$

where $m = 2k - nB$. From Eq. (A6) the upstream and downstream modal amplitudes [Eq. (23)] are readily identified.

Acknowledgment

The author gratefully acknowledges the improvements resulting from constructive comments in the reviews of the first version of this paper.

References

[1]Tyler, J. M., and Sofrin, T. G., "Axial Flow Compressor Noise Studies," *SAE Transactions*, Vol. 70, 1962, pp. 309–332.

[2]Schulten, J. B. H. M., "Vane Stagger Angle and Camber Effects in Fan Noise Generation," *AIAA Journal*, Vol. 22, No. 8, 1984, pp. 1071–1079.

[3]Katzmayr, R., "Effect of Periodic Changes in Angle of Attack on Behavior of Airfoils," *Zeitschrift für Flugtechnik und Motorluftschiffahrt*, 31 March and 13 April 1922, pp. 80–82, 95–101; see also NACA TM-147, 1922 (in English).

[4]Ribner, H. S., "Thrust Imparted to an Airfoil by Passage Through a Sinusoidal Upwash Field," *AIAA Journal*, Vol. 31, No. 10, 1993, pp. 1863–1868.

[5]Amiet, R. K., "Airfoil Leading-Edge Suction and Energy Conservation," *Journal of Fluid Mechanics*, Vol. 289, April 1995, pp. 227–242.

[6]Schulten, J. B. H. M., "Effects of Asymmetric Inflow on Near-Field Propeller Noise," *AIAA Journal*, Vol. 34, No. 2, 1996, pp. 251–258.

[7]Ffowcs Williams, J. E., and Hawkings, D. L., "Sound Generation by Turbulence and Surfaces in Arbitrary Motion," *Philosophical Transactions of the Royal Society of London, Series A*, Vol. 264, 1969, pp. 321–341.

[8]Schulten, J. B. H. M., "Advanced Propeller Performance Calculation by a Lifting Surface Method," *Journal of Propulsion and Power*, Vol. 12, No. 3, 1996, pp. 477–485.

[9]Schulten, J. B. H. M., "Vane Sweep Effects on Rotor/Stator Interaction Noise," *AIAA Journal*, Vol. 35, No. 6, 1997, pp. 945–951.

[10]von Kármán, T., and Burgers, J. M., "General Aerodynamic Theory—Perfect Fluids," *Aerodynamic Theory*, edited by W. F. Durand, Vol. 2, Springer, Berlin, 1935.

[11]Batchelor, G. K., *An Introduction to Fluid Dynamics*, Cambridge Univ. Press, Cambridge, England, U.K., 1967.

[12]Liepmann, H. W., and Puckett, A. E., *Introduction to Aerodynamics of a Compressible Fluid*, Wiley, New York, 1947.

[13]Polhamus, E. C., "A Concept of the Vortex Lift of Sharp-Edge Delta Wings Based on a Leading-Edge-Suction Analogy," NASA TN D-3767, 1966.

[14]Lamar, J. E., "Prediction of Vortex Flow Characteristics of Subsonic and Supersonic Speeds," *Journal of Aircraft*, Vol. 13, No. 7, 1976, pp. 490–494.

[15]Schlichting, H., *Boundary Layer Theory*, McGraw–Hill, New York, 1979, Chap. 24.

[16]Morfey, C. L., "Sound Generation in Ducts with Flow," *Journal of Sound and Vibration*, Vol. 14, No. 1, 1971, pp. 37–55.

[17]Schulten, J. B. H. M, "Sound Transmission Through a Rotor," *Proceedings of the Deutsche Gesellschaft für Luft- und Raumfahrt/AIAA 14th Aeroacoustics Conference*, Vol. 1, Deutsche Gesellschaft für Luft- und Raumfahrt, Bonn, 1992, pp. 502–509.

P. J. Morris
Associate Editor